nature geoscience

ARTICLES

PUBLISHED ONLINE: 9 SEPTEMBER 2012 | DOI: 10.1038/NGEO1562

Evolution of Santorini Volcano dominated by episodic and rapid fluxes of melt from depth

Michelle M. Parks[1], Juliet Biggs[2], Philip England[1], Tamsin A. Mather[1], Paraskevi Nomikou[3], Kirill Palamartchouk[1,4], Xanthos Papanikolaou[5], Demitris Paradissis[5], Barry Parsons[1], David M. Pyle[1]*, Costas Raptakis[5] and Vangelis Zacharis[5]

Santorini Volcano, the site of the catastrophic Minoan eruption in Greece, exhibits two distinct eruptive styles: small, effusive eruptions occur relatively frequently and build shields and domes of lava, whereas large explosive eruptions occur rarely, at intervals of 10,000–30,000 years. Both types of eruption were thought to incubate in a shallow magma chamber that is continually charged by small batches of melt injected into the chamber from below. However, petrological work suggests that at least 15% of the material ejected during the Minoan explosive eruption arrived in the magma chamber less than 100 years before the eruption. Here we use Satellite Radar Interferometry (InSAR) and Global Positioning System (GPS) measurements of surface deformation at Santorini to show that 10–20 million m^3 of magma have been intruded beneath the volcano since January 2011. This volume is equivalent to 10–50% of the volumes of recorded dome-forming eruptions. GPS and triangulation data show that this is the only volumetrically significant intrusion to have occurred since 1955, shortly after the last eruption. Our observations imply that whether Santorini is in an explosive or dome-forming phase, its shallow magma chamber is charged episodically by high-flux batches of magma. The durations of these events are short in comparison with the intervening periods of repose and their timing is controlled by the dynamics of deeper magma reservoirs.

The Kameni Islands (Fig. 1) are the surface expression of a dacitic volcanic dome complex that has grown during the past 3,600 yr in the caldera of the Minoan eruption[2–4] of about 1600 BC (ref. 1). Mineral thermobarometry and experimental petrological studies show that the lavas of the Kameni dome completed their pre-eruptive storage in a shallow reservoir at pressures of about 100 MPa (3–4 km in depth)[3,5,6]. The lavas from each eruption include a minor component of more mafic magma that forms enclaves that are significantly more crystalline and vesicular than the bulk lavas[5]. Disequilibrium chemical gradients within olivine crystals in dacites of the AD 1925 eruption suggest that these melts arrived within a pre-existing magma chamber a month or less before the eruption[7], and feldspar crystals from the host lavas contain diffusive compositional gradients consistent with residence for less than 100–500 years in a shallow reservoir[8]. Textural observations of crystal-size distribution are also interpreted in terms of a persistent shallow reservoir topped up, in the decades before eruption, by magmas with varying phenocryst contents[9]. These observations have led to a model in which, during its dome-forming phase, Santorini is underlain at shallow depth (~4 km) by a persistent dacitic magma chamber, which is charged by frequent batches of mafic melt that are small compared with the volume of the chamber[3,6,7,10]. The disequilibrium and vesicularity in the mafic enclaves are taken to suggest that the latest batch of melt triggered eruption by releasing volatiles that caused buoyant overturning of the magma chamber[6,7,11].

This model has recently been challenged in ref. 12, in which it is argued that, in the preparation phase for the Minoan eruption, the shallow magma chamber was charged by an event that contributed at least 15% of the erupted volume, in a time (about 100 years) that was very short in comparison with the interval since the previous major explosive eruption (18,000 years; ref. 4). Here we present evidence that, during its present dome-forming phase, the volcano is also charged by short-lived events, each of which contributes a significant fraction of the eventual erupted volume.

Historical eruptions and inflation of Santorini since 2011

Most of the post-Minoan edifice in the caldera of Santorini is submarine, but since AD 1570 five subaerial eruptions have formed the island of Nea Kameni (Table 1). The volumes of those eruptions (each a few times 10^7 to 10^8 m^3) are proportional to the repose period between them, as are the durations (1–4 years) of the eruptions themselves[13]. Both the volume of the dome built since the Minoan eruption (about 2.5 km^3 in 3,600 years) and the volume erupted since AD 1570 ($1.5–4 \times 10^8$ m^3) are equivalent to a time-averaged flux of between 0.5 and 1×10^6 m^3 yr^{-1} (refs 4, 6,12,13). The most recent sizeable eruption on Santorini took place in 1939–1941 (Table 1); multiplication of the time interval since 1941 by the average magma flux yields an expected volume for the next eruption, if it were to occur in the next few years, of between 3 and 7×10^7 m^3. Our measurements indicate that a volume of magma towards the lower end of that range has arrived beneath the caldera of Santorini since a period of volcanic unrest began in January 2011.

The onset of the unrest was marked by an increase in the rate of micro-seismic activity beginning in January 2011; at the same time, the coordinates of continuous GPS stations operating on Santorini began to deviate from their longer-term average

[1]Department of Earth Sciences, University of Oxford, South Parks Road, Oxford, OX1 3AN, UK, [2]School of Earth Sciences, University of Bristol, Bristol, BS8 1RJ, UK, [3]Department of Geology and Geoenvironment, University of Athens, Athens, Nomikou GR-15784, Greece, [4]School of Civil Engineering and Geosciences, University of Newcastle, Newcastle upon Tyne, NE1 7RU, UK, [5]Higher Geodesy Laboratory, National Technical University, Athens, NTUA GR-15780, Greece. *e-mail: David.Pyle@earth.ox.ac.uk.

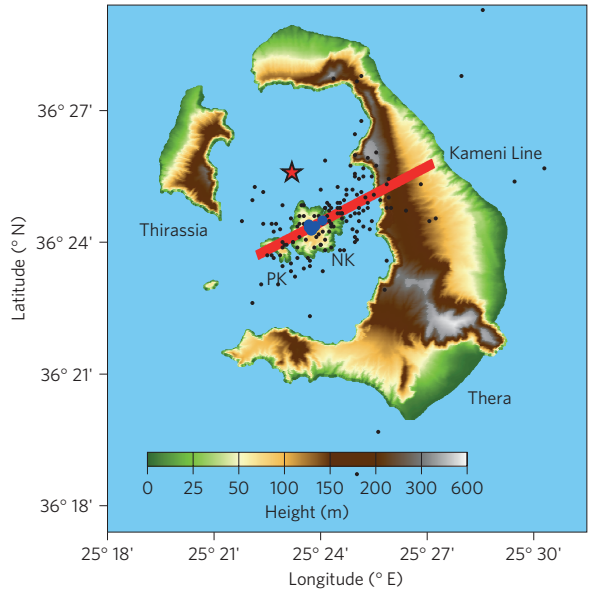

Figure 1 | The islands of the Santorini volcanic centre, and the location of the centre of recent volcanic and seismic activity. PK and NK denote the islands of Palaea and Nea Kameni, respectively; the Kameni Line[4], shown in red, passes through the locations of the vents of all the post-1570 eruptions (blue dots), and is probably an active normal fault that dips north-northwest. The red star shows the location of the centre of inflation deduced from the InSAR data reported here (Fig. 2). The black dots show epicentres of earthquakes of magnitude greater than two located by the Aristotle University of Thessaloniki[39] between January 2011 and April 2012. The present episode of volcanic unrest seems to have begun with three earthquakes of magnitude 1 on the 9 January 2011.

Table 1 | Timing and volumes of dome-forming eruptions on Nea Kameni since 1570, modified from ref. 13.

Eruption start date	Duration	Minimum volume (m^3)	GVP volume (m^3)
1570 or 1573	?	2.9×10^6	1.2×10^6
1707	$4\frac{1}{3}$ yr	1.1×10^7	8.1×10^7
1866	$4\frac{3}{4}$ yr	6.7×10^7	1.4×10^8
1925	9 months	2.5×10^7	10^8
1939	2 yr	4.3×10^7	6×10^7
(1950	23 d	6×10^5	7×10^4)
Total		1.5×10^8	3.8×10^8

Minimum volumes are estimated from the subaerial volumes of the flows, measured from a high-resolution digital elevation model[13]. GVP volumes are those quoted by the Global Volcanism Program of the Smithsonian Institution[40]. The eruption of 1950 is regarded as an appendix to the 1939–1941 eruption[13].

velocities[14]. We have used interferometric synthetic-aperture radar (InSAR) to measure ground deformation since March 2011 (Fig. 2 and Methods). We convert this signal into sub-surface volume increase by treating the displacements as arising from a pressure increase at a point within an elastic crust. Although the surface deformations at volcanoes may well result from complex distributions of sources at depth, such complexity is masked by the elasticity of the crust, which smooths disturbances over a horizontal scale comparable with their depth.

The simplest model, often referred to as a Mogi source, represents the magma chamber as a sphere whose radius is small compared with its depth[15,16]. We also investigated other simple sources: an ellipsoidal source[17–19] and a horizontal penny-shaped crack, representing a sill[20]. The ellipsoidal model produced fits that were indistinguishable from the spherical source. We found, as was found previously[14] for GPS data, that sill-shaped sources produce significantly poorer fits, and that it was not possible to resolve any finite-sized source. The quantity of importance to our argument is the volume of intruded magma, and the dominant uncertainties in that quantity are associated with compressibility of the magma, and the depth of the source, not with its shape. We therefore restrict discussion to the spherical source.

The best-fitting spherical source has an effective volume in the range $1–2\times10^7$ m^3, and is centred slightly to the north of Nea Kameni at a depth of $4.4^{+1.5}_{-1.1}$ km (Fig. 2 and Table 2). These estimates are similar to those obtained from GPS data up to December 2011 (ref. 14) except that the geometry of the InSAR observations allows us to place a tighter upper bound on the effective volume of the source than can be obtained from the GPS data (Fig. 3, Figure 3c of ref. 14 and Supplementary Information).

This effective volume represents a lower limit on the actual volume of magma intruded between January 2011 and April 2012. If the magma is entering an existing magma chamber then some of the intruded volume will be accommodated by compression of the surrounding magma, with a corresponding reduction in surface deformation (see ref. 21, p. 210). Under those circumstances, the effective volume calculated from displacements of the land surface ought to be multiplied by a factor of at least two and, if the magma contains volatiles in the gas phase, the multiplicative factor could be 5 or greater[21–23]. Nevertheless, in the following discussion, we use a figure of $1–2\times10^7$ m^3 for the intruded volume of magma, which is the range shown in Fig. 3; this would be an underestimate if the magma is entering a chamber that contains a significant volume of compressible magma.

Episodic rapid charging of the shallow magma chamber

We can place constraints on pre-2011 inflation of the volcano using earlier geodetic data. Electronic distance measurements taken between 1994 and 2000 suggest an inflationary episode of a few times 10^5 m^3 during that interval[24,25], which is negligible in comparison with the volume intruded in the present episode of inflation. A stronger constraint is provided by a triangulation survey of Santorini carried out in 1955. We re-occupied monuments of that survey in September 2011 using GPS. Displacements of the monuments between 1955 and September 2011 (Fig. 4a) are consistent with the ground deformation measured between January and September 2011; residuals (Fig. 4b) are a few centimetres in magnitude, consistent with uncertainties in the original triangulation, and show no systematic pattern. These observations imply either that there was no significant inflation of Santorini between 1955 and the beginning of 2011, or that any ground deformation that did take place was subsequently reversed to within a window of a couple of centimetres.

Since 1570, the interval between significant eruptions of Santorini has ranged from 14 to 160 years. It has been 70 years since the last significant eruption, and it is therefore prudent to consider whether the present unrest might presage the next eruption. The history of the volcano suggests that, if the present rate of inflation were to continue for a small number of years, the intruded volume would be equivalent to the volumes of previous eruptions (Table 1). The significant eruptions of last century had volumes of $4–6\times10^7$ m^3 (1939–1941) and $2.5–10\times10^7$ m^3 (1925–1926); if an eruption were to occur in the next few years, its expected volume, on the basis of long-term rates of eruption[13], would be between 3 and 7×10^7 m^3. Our range of estimates of the volume intruded since the beginning of 2011 is equivalent to 15–60% of that volume. It is known that many episodes of inflation at caldera-forming volcanoes do not end in eruption (for example, refs 26–28); on the other hand, dome-forming eruptions at Montserrat are preceded

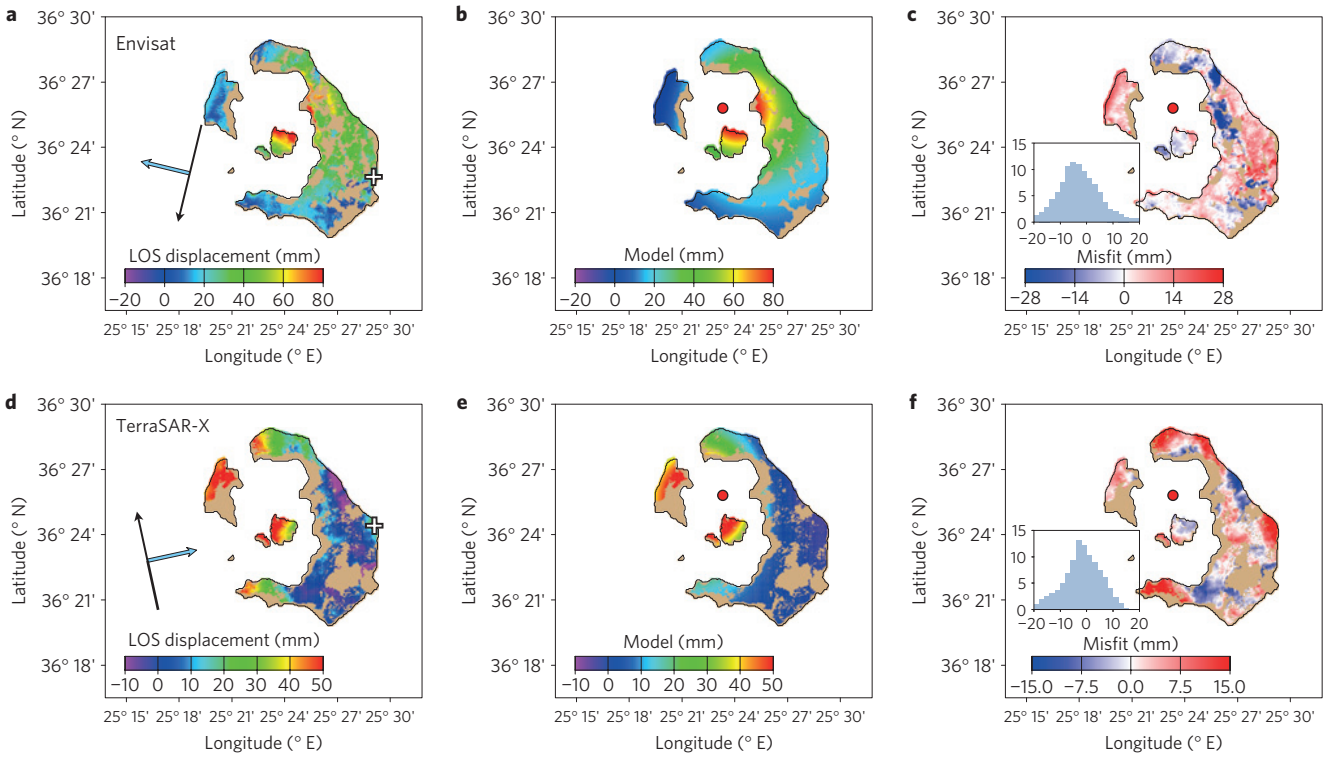

Figure 2 | InSAR measurements, and fits to them of the best-fitting spherical inflationary source, whose parameters are given in Table 2. **a**, Chain-stacked Envisat interferogram from 3 March to 28 December 2011; brown shading shows areas of land that were de-correlated. Thin arrow indicates orientation of satellite orbit, and thick arrow indicates the look direction of the satellite. Colours show ground displacement in the direction from the ground to the satellite. **b**, Calculated line-of-sight displacements for best-fitting spherical point source[15], which is at a depth of 4.4 km below the red dot (see Table 2). **c**, Misfits between best-fitting model (**b**) and the Envisat interferogram (**a**); inset histograms shows the distribution of misfits. **d**,**e**,**f**, As **a**, **b**, **c**, for chain-stacked TerraSAR-X interferograms from 25 July 2011 to 14 April 2012.

Table 2 | Best-fitting spherical sources[15] to interferogram stacks (Fig. 2).

	TerraSAR-X	Envisat	Estimate	Total
Time interval	25 July 2011–14 April 2012	3 March 2011–28 December 2011	9 January 2011–3 March 2011	9 January 2011–14 April 2012
Heading/incidence	−12.2°/39.5°	−166.4°/39.2°		
Wavelength (mm)	31	56		
Volume ($\times 10^6$ m^3)	8.8	9.5	1.6	14.9^{+7}_{-3}
Rate ($\times 10^3$ m^3 d^{-1})	33	32	(32)	32
r.m.s. misfit (mm)	7.3	6.2	-	6.8
	Location	25.389° E	36.430° N	Depth $4.4^{+1.1}_{-1.0}$ km

The bounds on depth and volume are derived from the trade-off between depth and volume of the source (Fig. 3). The inflation between January and March 2011 is calculated from the daily rate given by the Envisat stack which is shown in parentheses.

by 10–20 cm of uplift[29]—similar to the uplift on Santorini since January 2011. We therefore consider that it would be unwise to assume that the present state of unrest will not end in an eruption, although, at the time of writing, there is no indication that an eruption is imminent.

Our geodetic observations, which span 56 of the 70 years since the last sizeable eruption of Santorini, provide an unusual and perhaps unique example of long-term measurement of the surface deformation of a large silicic caldera that also has a centuries-long historical record of eruption. They strongly suggest that the present episode of volcanic inflation is the only significant one since the eruption of 1939–1941, or shortly thereafter. The volume intruded since the beginning of 2011 is of the same order of magnitude as the volumes of historical dome-forming eruptions. We therefore suggest that, during the dome-forming phase of its evolution, the shallow magma chamber beneath Santorini is charged by infrequent short-lived intrusive events, each of which delivers a significant fraction of the eventual erupted volume.

Magmatic evolution controlled by deeper reservoirs

Existing models envisage that the shallow magma chamber beneath Santorini is recharged by many small batches of andesitic melt, which fractionate within this reservoir to yield the more silicic magmas that finally erupt (for example, refs 3,7). Recently, it was argued[12] that the magma charging the shallow reservoir immediately before the Minoan eruption was predominantly silicic: a dacite-to-rhyolite magma formed by fractional crystallization at greater depths. We suggest that this also holds true for the present magmatic system. The erupted products of the Kameni domes consist almost entirely of homogeneous dacites[3,5]; the mafic

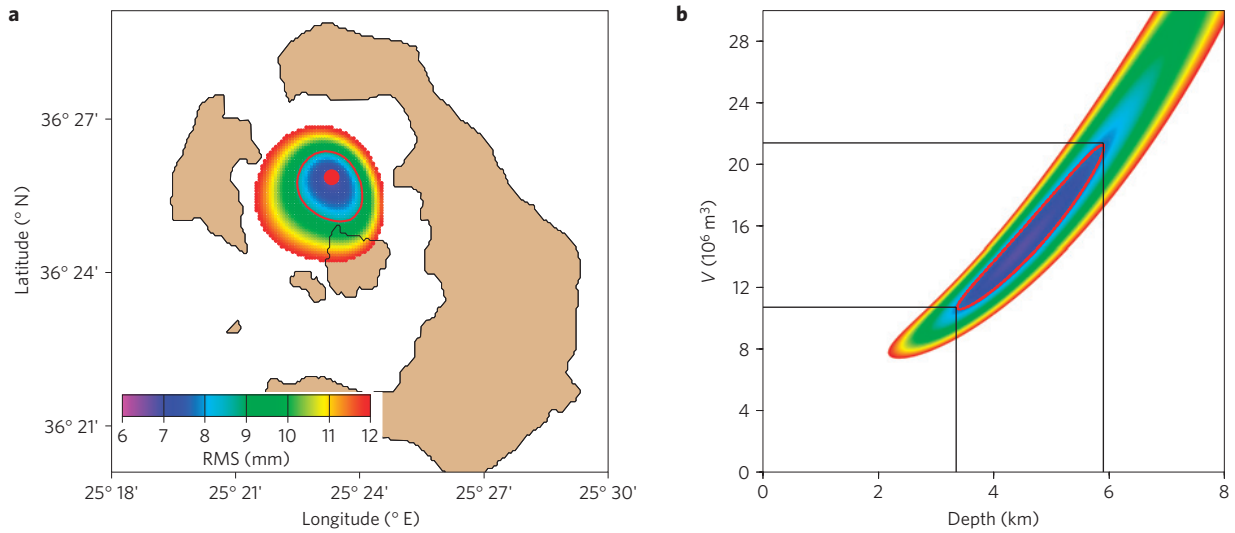

Figure 3 | Bounds on the location and volume of the magma body intruded beneath Santorini since January 2011. a, The colours show the minimum r.m.s. misfit between modelled and observed interferograms for spherical sources[15] beneath each location; where no colour is shown the r.m.s. misfit exceeds 12 mm. **b**, Trade-off between the depth of the spherical source and its effective volume. The colours (same scale as in **a**) show the r.m.s. misfit between observed and modelled interferograms with the depth and effective volume fixed at their respective values. The black lines correspond to the limits on source depth and effective volume given in Table 2. Effective volumes are calculated as described in the Methods; actual volumes could be considerably larger if the magma is entering an existing magma chamber (see text). Bounds on source location, depth and strength are shown by the red contours; solutions outside those contours show systematic misfits to the data (see Supplementary Information).

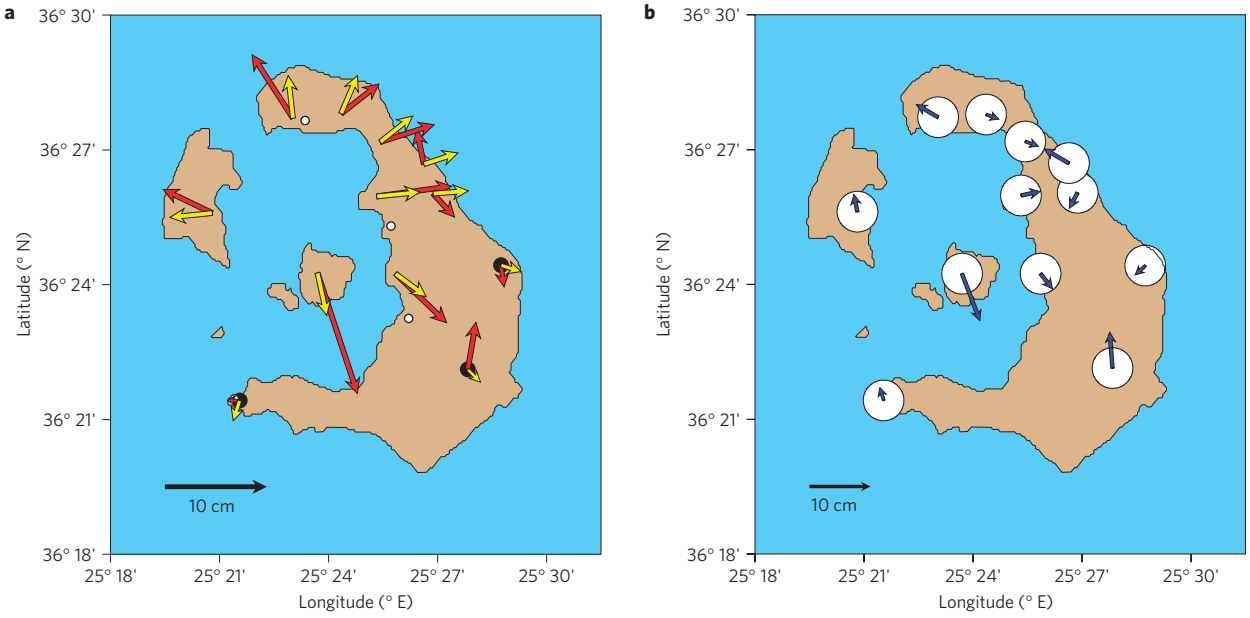

Figure 4 | Horizontal surface displacements of Santorini between 1955 and 2011 from triangulation and GPS data. a, The yellow vectors show the expected displacements if the only deformation in that time interval is that due to the inflation detected since the beginning of 2011 (Table 2). The red vectors show displacements of monuments between 1955 and 2011, calculated from measurements of angle made in 1955 and coordinates determined in 2011 using GPS. The white circles show the locations of continuous GPS sites used in GPS processing. The scale of the network in 1955 is determined using the points indicated by black circles (Methods). **b**, The blue vectors show the differences between the model (yellow in **a**) and observed (red) displacements; these represent displacements of the monuments between 1955 and the beginning of the volcanic unrest in January 2011. Uncertainties in triangulation measurements are discussed in the Methods, and are equivalent to 20 mm in each horizontal coordinate, as shown by the white circles.

(basaltic-andesitic) enclaves form less than 1% of the volume[6]. Although the model of a persistent shallow magma chamber recharged by many small batches of mafic melt is consistent with these observations, it is not demanded by them. Our data contradict the temporal aspect of that model, by showing that the shallow chamber is charged by infrequent large batches of magma; indeed, it is possible that the shallow magma chamber exists only in the relatively short interval (a year to a few years) immediately before dome-forming eruptions occur. The episodic nature of the recharging also casts doubt on the compositional aspect of the present model, because it is difficult to explain the observed petrological relationships if these infrequent charges of melt are mafic. If that were the case, the composition of the magma chamber would evolve episodically, as each large batch of melt

arrived and fractionated, with the last batch needing to fractionate almost completely (leaving a very small fraction of mafic enclaves) in the short time before eruption[7]. A simpler alternative is that the batches of melt reaching the shallow magma chamber are already dacitic in composition.

The major explosive eruptions of Santorini produce volumes of ejecta that range from $\sim 10^9$ to $\sim 5 \times 10^{10}$ m^3 (ref. 4), whereas the dome-forming eruptions are in the range $\sim 10^7$ to 10^8 m^3. Despite the great disparity between these scales, there are fundamental similarities in the behaviour of the volcanic system in these two phases of eruptive activity. In each case, the high-flux events charging the shallow magma chamber are dacitic in composition, they contribute a significant fraction (some tens of per cent) of the final erupted volume, and the durations of those events are short in comparison with the intervals of repose that separate them. Our observations, combined with those of ref. 12, strongly suggest that these similarities arise because, during either phase of its eruptive activity, the evolution of the shallow magma chamber beneath Santorini is regulated by the release of magma from a deeper reservoir, or reservoirs. Petrological evidence from the products of a number of eruptions on Santorini shows that such a reservoir exists at a depth of 10–14 km (refs 30–32).

These observations also suggest that the dynamics of the deep reservoirs are more intimately linked to eruption processes than has hitherto been recognized. The relations between the mafic enclaves and the host dacite have been taken to imply that small volumes of gas-rich mafic melt can trigger eruption from a shallow magma chamber[6,7,11]; this argument is still feasible, but it may apply to a deeper reservoir, rather than to the shallow chamber. Furthermore, the short timescales recorded by the disequilibrium chemical gradients in the lavas, previously thought to represent residence in the shallow magma chamber[7–9], probably represent the time taken for the large batches of dacitic magma to travel from a deep reservoir to the surface, including storage in the shallow chamber before eruption.

Although the historical record suggests that dome-forming eruptions last for only a few years (Table 1), the deep magmatic system is capable of delivering pulses that can last for the order of a century[12]. We are not aware of a mechanism that would restrict the deeper chamber to delivering a bimodal distribution of pulse durations (years or centuries); pulses of decadal duration may therefore also be expected, so future eruptions of Santorini will not necessarily be restricted to the range seen in the 500-year historical record. The need to acquire a better understanding of these processes is reinforced by the fact that the present episode of magma supply to the shallow chamber has a duration comparable to that of historical eruptions.

Methods

InSAR measurements. We measured the surface deformation on Santorini using InSAR analysis on data from the Envisat and TerraSAR-X satellites (Table 2), and a 15-m digital elevation model provided by P. Moore of IntegralGIS. We chain-stacked[33] the interferograms so that atmospheric noise on individual dates cancels out. Having obtained an approximate location for the source, we reduced the number of observations by forming averages that were equally spaced in distance (100 m) and azimuth (π/50 rad) from the source location. Rectangular grids with spacing between 200 and 500 m yielded results indistinguishable from those shown in Fig. 2.

As the area of interest consists of four islands, there is a potential ambiguity of an integer number of half-wavelengths in the displacements of the three smaller islands relative to Thera. However, the ground displacements between successive interferograms were small compared with half a wavelength, and the GPS data show no abrupt changes in deformation[14] so we were able to resolve the ambiguities by assuming monotonic, minimal, displacement of each island. This assumption was checked *a posteriori* by inspecting the residuals of each island to the best-fitting models; no island in either interferogram exhibited a misfit compatible with even a single half-wavelength offset (28 mm for Envisat or 16 mm for TerraSAR-X: each large in comparison with the root mean squared (r.m.s.) misfit of about 7 mm).

We calculated the location and volume of the intrusion from the interferograms using a spherical source[15,16]. We searched a rectangular mesh of spacing 100 m in all three dimensions, covering the plausible range of source locations. At each point, we solved for the best-fitting source strengths for the 300-day Envisat stack and for the 264-day TerraSAR-X stack, and for the offset of the reference points on Thera (Fig. 2). This procedure yielded an estimate for the volumes intruded during the (overlapping) time intervals covered by each interferogram stack; the rates of volume increase agreed between the two time intervals to within a few per cent (Table 2). We estimated the inflation between 25 July 2011 and 28 December 2011 (the period of overlap of the two interferogram stacks) by using the average of the rates of volume increase; outside that interval, we used the individual rates. We estimated the volume increase between the beginning of January 2011 and the first radar image on 03 March 2011 using the rate obtained for the Envisat stack. The results of this analysis are shown in Table 2.

Triangulation and GPS measurements. Triangulation observations were carried out on Santorini by the Hellenic Military Geographic Service in 1955. Each angle was the subject of a minimum of 12 independent measurements. In 1955 these observations were combined with assumptions of scale and orientation, by standard methods that have not changed[34], to yield a solution for coordinates (latitude, longitude and orthometric height); for comparison with GPS data, we subtracted the geoidal height[35] from the orthometric height.

Twelve of the original monuments on Santorini survive in usable condition, and we occupied these with GPS between 23 and 26 September 2011 (Fig. 4). The data from these sites, and from four continuous GPS sites on Santorini (whose locations are shown on Fig. 4), were analysed using Bernese v5.0 GPS software[36]. Coordinates were estimated in an ambiguity-fixed solution, using absolute antenna calibration corrections and International GNSS Service (IGS) final products[37]. The datum was realized by means of minimum constraints, imposed on IGS stations BOR1, BUCU, GLSV, ISTA, MATE, NICO, NOT1, PENC and WTZR. The processing was compliant with present Center for Orbit Determination in Europe (CODE) standards[38].

Owing to the imprecision of distance measurements of the time, the 1955 network contains an undetermined scale error, which we solved for as follows. We took the three points most distant from the centre of inflation (identified on Fig. 4) and subtracted from their 2011 coordinates the displacements calculated from our model for the inflation (spherical solution, Table 2, scaled for January–September, 2011). This adjustment is small in comparison with the motions of points nearer the source, because displacements decay as the square of distance from the source. We then found the isotropic horizontal dilatation to the 1955 coordinates that provided the best fit, in the least-squares sense, to the lengths of the baselines between these points in the adjusted 2011 coordinates. Finally, we oriented the 1955 network by finding the rigid-body rotation that produced the best fit to the calculated displacement vectors.

Although the original angular measurements were made using Wild T2 theodolites, which can measure to half a second of arc, which is equivalent to 10 mm over a typical side length of 5 km in the triangulation, we adopt a conservative estimate of 20 mm for the uncertainty in positions of the original coordinates. We (D.P., C.R. and X.P.) have compared many triangulation surveys with GPS observations in the past 15 years, and have found that relative coordinates based on terrestrial measurements are generally accurate to the order of 10–20 mm.

Received 26 March 2012; accepted 3 August 2012; published online 9 September 2012

References

1. Friedrich, W. *et al.* Santorini eruption radiocarbon dated to 1627–1600 BC. *Science* **312,** 548–548 (2006).
2. Fouqué, F. *Santorin et ses éruptions*(Masson et Cie 1879) (Translation: McBirney, A. R. *Santorini and Its Eruptions by Ferdinand Fouqué* (Johns Hopkins Univ. Press 1998).
3. Barton, M. & Huijsmans, J. Post-caldera dacites from the Santorini volcanic complex, Aegean Sea, Greece: An example of the eruption of lavas of near-constant composition over a 2200 year period. *Contrib. Mineral. Petrol.* **94,** 472–495 (1986).
4. Druitt, T. H. *et al. Santorini Volcano Vol. 19* (Geol. Soc. Lond. Memoir, 1999).
5. Nicholls, I. A. Petrology of Santorini volcano, Cyclades, Greece. *J. Petrol.* **12,** 67–119 (1971).
6. Martin, V., Holness, M. & Pyle, D. Textural analysis of magmatic enclaves from the Kameni Islands, Santorini, Greece. *J. Volcanol. Geotherm. Res.* **154,** 89–102 (2006).
7. Martin, V. *et al.* Bang! month-scale eruption triggering at Santorini volcano. *Science* **321,** 1178 (2008).
8. Zellmer, G., Blake, S., Vance, D., Hawkesworth, C. & Turner, S. Plagioclase residence times at two island arc volcanoes (Kameni Islands, Santorini, and Soufrière, St. Vincent) determined by Sr diffusion systematics. *Contrib. Mineral. Petrol.* **136,** 345–357 (1999).

9. Higgins, M. D. Magma dynamics beneath Kameni volcano, Thera, Greece, as revealed by crystal size and shape measurements. *J. Volcanol. Geotherm. Res.* **70,** 37–48 (1996).
10. Mann, A. Trace-element geochemistry of high alumina basalt-andesite-dacite-rhyolite lavas of the main volcanic series of Santorini volcano, Greece. *Contrib. Mineral. Petrol.* **84,** 43–57 (1983).
11. Sparks, R., Sigurdsson, H. & Wilson, L. Magma mixing—mechanism for triggering acid explosive eruptions. *Nature* **267,** 315–318 (1977).
12. Druitt, T. H., Costa, F., Deloule, E., Dungan, M. & Scaillet, B. Decadal to monthly timescales of magma transfer and reservoir growth at a caldera volcano. *Nature* **482,** 77–80 (2012).
13. Pyle, D. & Elliott, J. Quantitative morphology, recent evolution, and future activity of the Kameni Islands volcano, Santorini, Greece. *Geosphere* **2,** 253–268 (2006).
14. Newman, A. V. *et al.* Recent geodetic unrest at Santorini Caldera, Greece. *Geophys. Res. Lett.* **39,** L06309 (2012).
15. Mogi, K. Relations between the eruptions of various volcanoes and the deformations of the ground sources around them. *Bull. Earthq. Res. Inst. Jpn* **36,** 99–134 (1958).
16. McTigue, D. F. Elastic stress and deformation near a finite spherical magma body: resolution of the point source paradox. *J. Geophys. Res.* **92,** 12931–12940 (1987).
17. Davis, P. Surface deformation due to inflation of an arbitrarily oriented triaxial ellipsoidal cavity in an elastic half-space, with reference to Kilauea volcano, Hawaii. *J. Geophys. Res.* **91,** 7429–7438 (1986).
18. Yang, X-M., Davis, P. M. & Dieterich, J. H. Deformation from inflation of a dipping finite prolate spheroid in an elastic half-space as a model for volcanic stressing. *J. Geophys. Res.* **93,** 4249–4257 (1988).
19. Newman, A., Dixon, T. & Gourmelen, N. A four-dimensional viscoelastic deformation model for Long Valley caldera, California, between 1995 and 2000. *J. Volcanol. Geotherm. Res.* **150,** 244–269 (2006).
20. Sun, R. Theoretical size of hydraulically induced horizontal fractures and corresponding surface uplift in an idealized medium. *J. Geophys. Res.* **74,** 5995–6011 (1969).
21. Segall, P. *Earthquake and Volcano Deformation* (Princeton Univ. Press, 2010).
22. Rivalta, E. & Segall, P. Magma compressibility and the missing source for some dike intrusions. *Geophys. Res. Lett.* **35,** L04306 (2008).
23. Mastin, L. G., Roeloffs, E., Beeler, N. M. & Quick, J. E. in *A Volcano Rekindled: The Renewed Eruption of Mount St Helens, 2004–2006* (eds Sherrod, D. R., Scott, W. E. & Stauffer, P. H.) Ch. 22, 462–488 (US Geological Survey, 2008).
24. Stiros, S. C., Psimoulis, P., Vougioukalakis, G. & Fyticas, M. Geodetic evidence and modeling of a slow, small-scale inflation episode in the Thera (Santorini) volcano caldera, Aegean Sea. *Tectonophysics* **494,** 180–190 (2010).
25. Saltogianni, V. & Stiros, S. C. Modeling the Mogi magma source centre of the Santorini (Thera) volcano, Aegean Sea, Greece, 1994-1999, based on a numerical-topological approach. *Stud. Geophys. Geod.* **56** http://dx.doi.org/10.1067/s11200-012-0408-z (2012).
26. Chang, W-L., Smith, R.B., Farrell, J. & Puskas, C. An extraordinary episode of Yellowstone caldera uplift, 2004-2010, from GPS and InSAR observations. *Geophys. Res. Lett.* **37,** L23302 (2010).
27. Fournier, T. J., Pritchard, M. E. & Riddick, S. N. Duration, magnitude, and frequency of subaerial volcano deformation events: New results from Latin America using InSAR and a global synthesis. *Geochem. Geophys. Geosyst.* **11,** Q01003 (2010).
28. Liu, Z., Dong, D. & Lundgren, P. Constraints on time-dependent volcanic source models at Long Valley caldera from 1996 to 2009 using InSAR and geodetic measurements. *Geophys. J. Int.* **187,** 1283–1300 (2011).
29. Mattioli, G. S. *et al.* Long term surface deformation of Soufrière Hills volcano, Montserrat from GPS geodesy: Inferences from simple elastic inverse models. *Geophys. Res. Lett.* **37,** L00E13 (2010).
30. Cottrell, E., Gardner, J. & Rutherford, M. Petrologic and experimental evidence for the movement and heating of the pre-eruptive Minoan rhyodacite (Santorini, Greece). *Contrib. Mineral. Petrol.* **135,** 315–331 (1999).
31. Gertisser, R., Preece, K. & Keller, J. The Plinian Lower Pumice 2 eruption, Santorini, Greece: Magma evolution and volatile behaviour. *J. Volcanol. Geotherm. Res.* **186,** 387–406 (2009).
32. Andújar, J., Scaillet, B., Pichavant, M. & Druitt, T. H. Differentiation conditions of a basaltic magma from Santorini and its bearing on andesitic/dacitic magma production. *Eos. Trans. AGU (Fall Meeting Suppl.)* abstr. #V43A-2354 (2010).
33. Biggs, J., Wright, T., Lu, Z. & Parsons, B. Multi-interferogram method for measuring interseismic deformation: Denali Fault, Alaska. *Geophys. J. Int.* **170,** 1165–1179 (2007).
34. Bomford, G. *Geodesy* 4th edn (Oxford Univ. Press, 1980).
35. Pavlis, N., Holmes, S., Kenyon, S. & Factor, J. *EGM2008: An Earth Gravitational Model to Degree 2160* (General Assembly of the European Geosciences Union, 2008).
36. Dach, R., Hugentobler, U., Fridez, P. & Meindl, M. *Bernese GPS Software Version 5.0*, User Manual, Tech. Rep., (Astronomical Institute, Univ. Bern, 2007).
37. Dow, J., Neilan, R. E. & Rizos, C. The international GNSS service in a changing landscape of Global Navigation Satellite Systems. *J. Geodesy* **83,** 191–198 (2009).
38. http://igscb.jpl.nasa.gov/igscb/center/analysis/code.acn.
39. http://geophysics.geo.auth.gr/.
40. Siebert, L. & Simkin, T. *Volcanoes of the World: An Illustrated Catalog of Holocene Volcanoes and their Eruptions*, (Smithsonian Institution Digital Information Series GVP-3, http://www.volcano.si.edu/world 2002).

Acknowledgements

We are grateful to A. Newman and S. Stiros for sharing data and ideas. The Hellenic Military Geographical Service kindly provided us with their triangulation data for Santorini. We are grateful to E. Fielding for discussions, and to the JPL ROI_PAC team for development of the TSX reader. We thank the Santorini Bellonio library and I. Perros for providing access to historical documents. We thank A. Argirou, C. Kay, R. Neely, E. Warren-Smith and the 2011 Greek Field Class of the Department of Earth Sciences, University of Oxford, for their assistance in the field. During our fieldwork the Nomikos Foundation and the Boatmen Union of Santorini kindly provided transport. This work was supported by NERC through grant NE/J011436/1, and by a loan of equipment from its Geophysical Equipment Facility. The National Centre for Earth Observation (NCEO) provided support through a studentship to M.M.P. All TerraSAR-X data are copyrighted by the German Space Agency (DLR), which provided them under scientific proposal GEO1228. All Envisat SAR data are copyrighted by the European Space Agency, which provided them under project AOE621 and through an STSE fellowship to J.B. We thank P. Moore and M. Davis for providing the digital elevation model used in the InSAR processing.

Author contributions

J.B., P.E., T.A.M., D.P. and D.M.P. designed projects that, as a result of the volcanic unrest on Santorini, came together in this study. InSAR processing and analysis were undertaken by M.M.P. and J.B., and source modelling by P.E., J.B. and M.M.P. The re-occupation of old triangulation sites was coordinated by D.P. and carried out by D.P., C.R., V.Z., P.E., P.N. and M.M.P. Processing and interpretation of Greek triangulation network data were undertaken by D.P., C.R., X.N. and P.E. The GPS sites used in this study were installed by C.R., K.P. and B.P., and K.P. assisted in processing their data. P.E., M.M.P. and D.M.P. wrote the paper; all other authors then commented on and contributed to the final version.

Additional information

Supplementary information is available in the online version of the paper. Reprints and permissions information is available online at www.nature.com/reprints. Correspondence and requests for materials should be addressed to D.M.P.

Competing financial interests

The authors declare no competing financial interests.